ACS APPLIED MATERIALS & INTERFACES

Research Article

Cite This: ACS Appl. Mater. Interfaces 2018, 10, 36094−36101

www.acsami.org

Highly Conductive Fiber with Waterproof and Self-Cleaning Properties for Textile Electronics

Byungwoo Choi,[†] Jaehong Lee,[‡] Heetak Han,[†] Janghoon Woo,[†] Kijun Park,[†,§] Jungmok Seo,[*,§,∥] and Taeyoon Lee[*,†]

[†]Nanobio Device Laboratory, School of Electrical and Electronic Engineering, Yonsei University, 50 Yonsei-ro, Seodaemun-Gu, Seoul 03722, Republic of Korea

[‡]Laboratory of Biosensors and Bioelectronics, ETH Zürich, Gloriastrasse 35, 8092 Zurich, Switzerland

[§]Center for Biomaterials, Biomedical Research Institute, Korea Institute of Science and Technology, Hwarang-ro 14-gil 5, Seongbuk-gu, Seoul 02792, Republic of Korea

[∥]Division of Bio-Medical Science & Technology, KIST School, Korea University of Science and Technology (UST), Seoul 02792, Republic of Korea

Supporting Information

ABSTRACT: Major concerns in the development of wearable textile electronics are exposure to moisture and contamination. The exposure can cause electrical breakdown of the device and its interconnections, and thus continuous efforts have been made to fabricate textile electronics which are free from moisture and pollution. Herein, we developed a highly conductive and waterproof fiber with excellent electrical conductivity (0.11 Ω/cm) and mechanical stability for advanced interconnector components in wearable textile electronics. The fabrication process of the highly conductive fiber involves coating of a commercial Kevlar fiber with Ag nanoparticle−poly(styrene-*block*-butadiene-*block*-styrene) polymer composites. The fabricated fiber then gets treated with self-assembled monolayer (SAM)-forming reagents, which yields waterproof and self-cleaning properties. To find optimal SAM-forming reagents, four different kinds of reagents involving 1-decane thiol (DT), 1*H*,1*H*,2*H*,2*H*-perfluorohexanethiol, 1*H*,1*H*,2*H*,2*H*-perfluorodecyltrichlorosilane, 1*H*,1*H*,2*H*,2*H*-perfluodecanethiol (PFDT) were compared in terms of their thiol group and carbon chain lengths. Among the SAM-forming reagents, the PFDT-treated conductive fiber showed superior waterproof and self-cleaning property, as well as great sustainability in the water with varying pH because of nanoscale roughness and low surface energy. In addition, the functionality of the conductive fiber was tested under mechanical compression via repeated washing and folding processes. The developed conductive fiber with waterproof and self-cleaning property has promising applications in the interconnector operated under water and textile electronics.

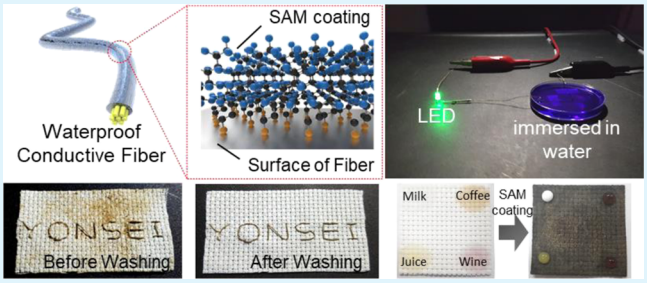

KEYWORDS: *wearable device, E-textile, conductive fiber, self-assembled monolayer, superhydrophobic, waterproof, washable, self-cleaning*

1. INTRODUCTION

Wearable devices, which are equipment that combine electronic devices with wearable items, have been developed extensively for various applications such as gesture recognition,[1] health monitoring,[2] energy harvesting,[3] and wireless communication[4,5] because of the outstanding benefits of intimate interactions between wearable devices and the user. More specifically, electronic textile (E-textile), which integrates electronic components into the form of fabrics, exhibits significant advantages because of its wearability and deformability.[6−8] To develop more advanced E-textile devices, the development of conductive fiber with a high electrical conductivity and mechanical durability that can be sustained under repeated stress motions and various conditions is fundamentally essential.[9,10] Recently, studies on conductive fibers have demonstrated progressive results in terms of such high electrical performance of the conductive fiber.[9−15] For example, Xu et al. fabricated a conductive fiber by using a polypyrrole-carbon nanotube composite.[14] The carbon nanotube composite fiber showed high conductivity above 10 kS/m with mechanical stability. Our group has recently demonstrated fine work of the conductive fiber using a silver (Ag)−polymer nanocomposite, which showed excellent electrical conductivity with superior mechanical durability.[9,10] Although the aforementioned conductive fiber showed great electrical and mechanical properties, they can be easily wetted and can

Received: June 19, 2018
Accepted: September 17, 2018
Published: September 17, 2018

DOI: 10.1021/acsami.8b10217
ACS Appl. Mater. Interfaces 2018, 10, 36094−36101

lose their electrical conductivity in operations, which hinder its practical applications. Furthermore, wet E-textile can cause electrical hazards such as performance degradation, electrical shock to the user, or electrical breakdown of the electronic devices.

To solve the water-penetration issue, Yang et al. demonstrated a waterproof supercapacitor fabric by covering a supercapacitor core with a hydrophobic polyester outer layer.[16] However, such a multilayer encapsulation approach has a negative effect in terms of long-term stability and flexibility because of thickness and the mechanical mismatch of the encapsulation layer. In addition, such physical encapsulation can be easily penetrated by water causing the malfunction of E-textile devices. Soto et al. fabricated nonwetting coatings for the fabric material via initiated chemical vapor deposition of fluorinated polymers.[17,18] The coated fabric demonstrated a highly water-repellant surface, even maintaining its property after several washing processes. However, the fabric is composed of electrically nonconductive material, which is not adequate for E-textile applications. Wu et al. developed wash-durable, stretchable, and conductive fibers to monitor tiny motions of users.[19] A conductive polymer complex coated on a stretchable fiber exhibited wash-durable properties owing to the dense conformation of the conductive polymer complex composed of carbon black, cellulose nanocrystals, and natural rubber. Because of the chemical resistance of the natural rubber, the conductive polymer complex exhibited wash-durability against water, acids, and alkalis. Despite the wash-durability, the poor electrical conductivity (1.9 MΩ/cm) of the wash-durable conductive complex makes it not suitable for advanced E-textile applications. Recently, Jeon et al. fabricated a graphene oxide-silk composite conductive fiber.[20] The research shows stable electrical operation even after 10 times of washing cycle. However, the composite fiber demonstrates relatively low conductivity compared to the metal-based materials because of poor connectivity between carbon nanomaterials in the conductive fiber. Therefore, to develop advanced interconnectors for E-textiles, conductive fibers should maintain a suitable stability against wet conditions with superb electrical and mechanical properties.

In this study, we developed a facile method for the fabrication of a highly conductive and mechanically durable fiber with waterproof and self-cleaning properties. The high conductivity of the fiber can be achieved by coating a commercial fiber scaffold with a Ag nanoparticle (NP)−poly(styrene-*block*-butadiene-*block*-styrene) (SBS) polymer composite layer. The obtained conductive fiber exhibits a very low resistance (0.11 Ω/cm) and excellent physical durability against folding deformation repeated 10 000 times. Self-assembled monolayer (SAM) reagents with low surface energyare then vapor-deposited onto the conductive fiber for self-cleaning and waterproof properties. Because of the combination of nanoscale roughness and the low surface energy of the SAM, the excellent electrical conductivity is successfully retained after submersion in water, even in acidic and alkali solutions. The water-repellent fiber surface protects Ag NPs inside the SBS polymer composite layer of the conductive fiber from oxidation caused by water and other oxidative compounds. With this protective property, the waterproof conductive fiber could retain the high conductivity longer in humid or watery conditions than previous works of conductive fibers. Furthermore, the conductive fiber effectively repels and removes contaminants. As an interconnector material for E-textiles, the waterproof conductive fiber was used to operate a light emitting diode (LED) underwater. In addition, various tests including laundry washing test and AATCC (American Association of Textile Chemists and Colorists) tests were conducted to test the fiber's functionality when it is exposed to wetting conditions.

2. EXPERIMENTAL SECTION

2.1. Fabrication of an Electrically Conductive Layer on Commercial Kevlar Fiber and Commercial Textile. The commercially available Kevlar fiber (Grade I K49, 100D) is composed of a multifilament bundle of the Kevlar fiber, which has yellowish color. The Kevlar fiber is chosen as it exhibits exceptional modulus suitable for tough interconnector material. The fiber with a length of 15 cm and commercially available cross-stitch textile (canvas cloth) were cut into 3 × 3 cm^2 size. To make the samples perpendicular to the ground, they were hung on a stand with 100 g of weights, and 2 mL of SBS solution (10 wt %) dissolved in a mixed solvent of tetrahydrofuran and dimethylformamide (3:1) was released along the vertically hung Kevlar fibers and textiles. After 10 min of drying, the SBS-coated Kevlar fibers and textiles were immersed into a CF_3COOAg solution dissolved in ethanol (20 wt %) for 20 min to absorb Ag^+ ions into the polymer layer. After 10 min of drying, 50 wt % hydrazine hydrate ($N_2H_4{\cdot}4H_2O$) in a mixture with ethanol was released onto the fibers to reduce the Ag^+ ions in the polymer to Ag NPs. After 10 min, the residual reduction agent was washed several times using deionized water. Then, the fabrication process from the absorption of the CF_3COOAg solution and exposure to hydrazine hydrate was repeated eight times.

2.2. Vapor Deposition of SAM Reagents. For the formation of SAMs onto the conductive fiber and textile samples, we used various SAMs such as 1-decane thiol (DT), 1*H*,1*H*,2*H*,2*H*-perfluorohexanethiol (PFHT), 1*H*,1*H*,2*H*,2*H*-perfluorodecyltrichlorosilane (FDTS), 1*H*,1*H*,2*H*,2*H*-perfluodecanethiol (PFDT). All SAMs were purchased at Sigma-Aldrich and used them as received. The conductive fibers and textiles were placed in a vacuum chamber (10^{-1} Pa) with 1 mL of SAM reagents. The chamber was heated at 50 °C for 2 h for the vapor deposition of SAM reagents onto the samples. Then, the samples were annealed at 80 °C for 30 min.

2.3. Confocal Microscopic Measurements for Wetting Behavior Characteristic of Conductive Fibers. Rhodamine 6G (R6G, Sigma-Aldrich) was used as probing molecules for confocal microscopic measurements. Conductive fibers without SAMs and conductive fibers with PFDT were submerged for 10 s into a 10^{-4} M R6G solution. After 30 min of drying, confocal microscopic measurements were performed using a Carl Zeiss LSM 880 confocal microscope.

2.4. Laundry Washing Process on Conductive Fiber-Woven Fabrics. The conductive fiber with and without the PFDT layer was woven into a fabric of the 1/1 structure. Then, the conductive fabric was contaminated using sand dust. For the washing process, 25 g of the commercial liquid laundry detergent (Tech, LG life science, Korea) was poured into 500 mL of water. The woven fabric was placed in water and stirred at a temperature of 10 °C for 30 min and then dried.

2.5. AATCC Tests. Resistance of the conductive fiber-based fabric with the PFDT layer to wetting resistance was tested with various liquid combinations and water/isopropyl alcohol (IPA) solutions. AATCC 118 measures resistance of the fabric to various liquids solution including cooking oil, milk, coffee, wine, and orange juice on the fabric and the contamination level gets optically measured. AATCC 130 measures fabric's ability to release corn oil stains via laundry. In addition, AATCC 193 uses water/IPA solution of varying concentrations from 198:2 to 840:60 to measure the contact angle between the fabric and solution and its permeability.

2.6. Repeated Folding Deformation Test. The free-standing conductive fiber was fixed on the poly(ethyleneterephtalate) (PET) film with 0.2 mm thickness applying small amounts of silver paste and gold tape at both ends of the conductive fiber. Then, the fixed

DOI: 10.1021/acsami.8b10217
ACS Appl. Mater. Interfaces 2018, 10, 36094−36101

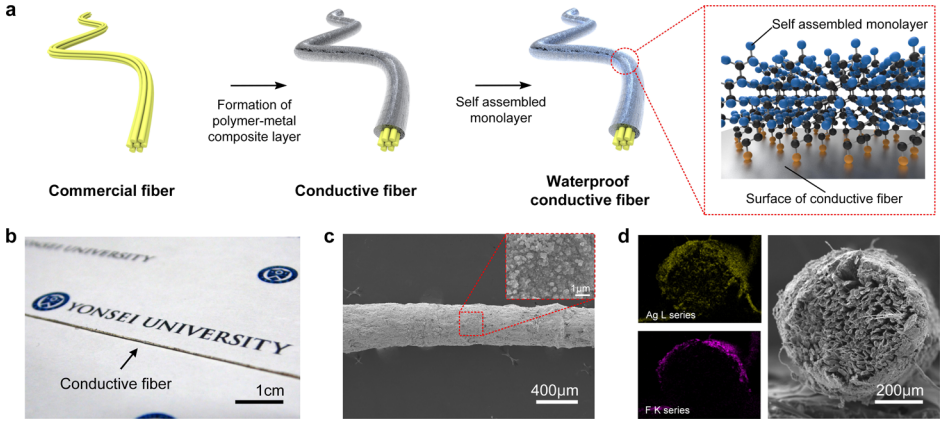

Figure 1. (a) Fabrication process of a waterproof conductive fiber. (b) Photographic image of the waterproof conductive fiber. (c) Typical SEM image of the waterproof conductive fiber and high magnification image (inset). (d) EDS analysis of Ag (upper left) and F (lower left) with a cross-sectional view of an SEM image (right side).

conductive fiber was placed on the X-stage motion controller (ST1, Korea). The PET film only supports the free-standing conductive fiber to make the folding motion more controllable, and thus, its effect on the folding results is negligible. Each movement of the folding or releasing was programmed to move for 3 s. In addition, the relaxation time is programmed for 1 s between folding and releasing. The resistance changes of fibers were measured by using Keithley 2400.

2.7. Characterization. Electron microscope and energy-dispersive spectroscopic (EDS) measurements were performed using a JEOL JSM-7800F field emission scanning electron microscope. Contact angle measurement was conducted with a FEMTOFAB SDS-TEZD contact angle measurement device. The Fourier transform infrared (FT-IR) spectrum was measured using a Bruker Vertex 70 FT-IR spectrometer. Thermogravimetric analysis (TGA) was performed using TA Instrument Q50. The surface morphology was examined using a JPK Nanowizard I atomic force microscope (AFM). X-ray diffraction was performed using a Rigaku Smartlab high-resolution X-ray diffractometer. X-ray photon spectroscopy (XPS) was examined using Thermo scientific K-alpha.

3. RESULTS AND DISCUSSION

Figure 1a shows a scheme of the fabrication process for the waterproof conductive fiber. The waterproof conductive fiber can be fabricated through two steps: the first step is the formation of a flexible and conductive layer on the surface of a commercialized Kevlar; the second step is the waterproof surface treatment of the conductive fiber by using SAM chemical reagents having different carbon chain lengths and head groups. Figure 1b shows a photograph of a waterproof conductive fiber, demonstrating its silvery-gray color coming from the formed Ag NPs. In comparison with the pristine Kevlar fiber, the conductive fiber exhibited an insignificant change in its diameter (from 0.2 to 0.3 mm) and weight (from 0.15 to 0.3 g/m) because of the addition of the conductive Ag NP-SBS polymer composite layer. Figure 1c shows a typical SEM image of the conductive fiber. As fluorocarbon molecules adsorb onto the metal surface of the conductive fiber and formed an electrically conducting path with high conductivity. The electrical performance of the conductive fiber can be enhanced by repeating the Ag precursor absorption and reduction process. Figure S1 shows the increase of electrical conductivity as increasing the repeat cycle. The resistance of the conductive fiber could be decreased to be 0.11 Ω/cm after eight repeated cycles of the absorption of Ag precursors and its reduction to Ag NPs. The high electrical performance results from the uniform and dense distribution of Ag NPs, which forms a conductive pathway inside the conductive fiber. To measure the amount of Ag NPs inside the polymer-composited conductive fiber, TGA analysis has been carried out. Figure S2 exhibits the results of the TGA for the conductive fibers according to the number of the absorption and reduction processes. The percentage of Ag NPs in the polymer-composited conductive fiber increased from 61.4 to 83.9 wt % as the number of incorporation process cycle increases. According to the TGA results, the repeated absorption and reduction of the Ag precursor caused greater generation of Ag NPs inside the SBS polymer composite layer of the conductive fiber. In the percolation theory,[10,15] the electrical conductivity of a conductive composite is determined by the electrical pathway of the closely located conductive particles. In the case of the developed waterproof conductive fiber, the dense and uniform distribution of Ag NPs produces an abundant electrical pathway that results in excellent electrical conductivity. Figure 1d presents EDS mapping images of the Ag L series and F K series for a cross-sectional view of the waterproof conductive fiber, respectively. The EDS mapping image of the Ag L series in the left-upper side shows a uniform distribution of the Ag NPs inside the SBS polymer composite layer among the intervals of the Kevlar filaments. The uniform distribution of Ag NPs inside the fiber results from the absorption process during the fabrication. In the absorption procedure, the Ag precursor was effectively absorbed into the SBS polymer layer, which is flowed into the intervals among the Kevlar filaments through an ion−dipole interaction between the trifluoroacetate anions (CF_3COO^-) and hydroxyl groups (−OH) of the alcoholic solvent.[9,21] In the left-lower side, the EDS mapping image of the F K series shows a high intensity of fluorine from the formed PFDT SAM along the surface of the waterproof conductive fiber. As SAM molecules which has fluorine atoms adsorb onto the metal surface of the conductive fiber, the EDS image shows the dense fluorine intensity.

Owing to the combination of the rough surface formed by SBS-Ag NP clusters with a SAM having a low surface energy, the surface of the waterproof conductive fiber exhibits improved waterproof property.[22,23] To characterize the waterproof property of SAM-coated conductive fibers, we coated four different types of SAM-forming reagents having different carbon chain lengths and head groups (DT, PFHT, FDTS, and PFDT). To observe the wetting characteristics and

DOI: 10.1021/acsami.8b10217
ACS Appl. Mater. Interfaces 2018, 10, 36094−36101

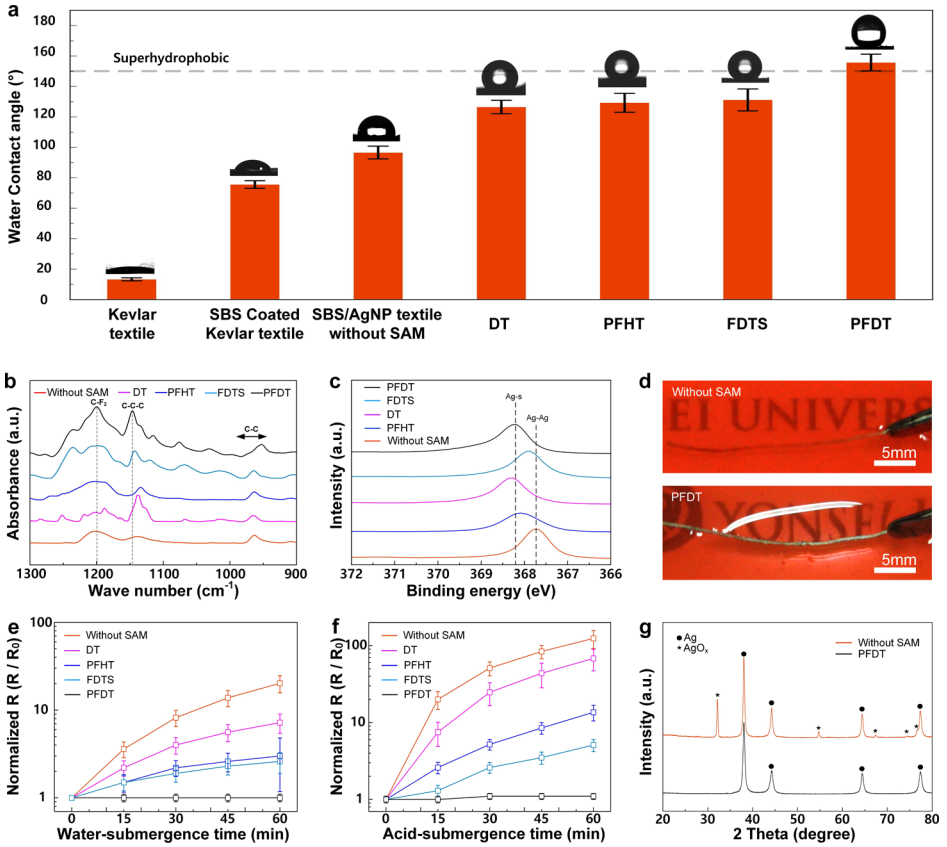

Figure 2. (a) Water contact angles on the Kevlar textile samples coated with different SAMs. (b) FT-IR analysis of the conductive fibers with different SAM reagents. (c) XPS analysis of the conductive fibers with different SAM reagents. (d) Photographic images of SAM-coated conductive fiber repelling dyed water. (e) Resistance changes of conductive fibers with different SAM reagents after water submergence. (f) Resistance changes of conductive fibers with different SAM reagents after acid submergence. (g) XRD analysis of the bare conductive fiber and PFDT SAM reagent-coated conductive fiber after 1 h of acid submergence.

the tendency of surface wettability against water, we formed the Ag NP-SBS polymer composite onto the weaved Kevlar fabric and measured water contact angle (Figure 2a). Compared to the pristine Kevlar fabric, both SBS-coated and AgNP-SBS composite-coated samples showed increased water contact angles because ofthe rough surface of the SBS polymer. The slightly higher water contact angle of the AgNP-SBS-composite coated layer is attributed to the Ag NPs-induced nanostructures on the surface. After SAM formation on the fabric surface, the water contact angle turns the hydrophobic region (over 90°) for all SAM reagents. Specifically, only the PFDT SAM layer shows a water contact angle over 150°, which means that the surface of the conductive fiber is superhydrophobic. The observed superhydrophobic property of PFDT-coated fibers is mainly attributed to the combination of the low surface energy and nanoscale roughness of the conductive fibers. According to the Cassie−Baxter wetting model, the wetting behavior of a water droplet on a rough surface is determined by assuming that the water droplet sits on air cushions between the water droplet and the rough surface.[24,25] In the model, the actual contact area between the rough surface and the water droplet decreases with increasing roughness, making the rough surface hydrophobic. Figure S3a,b shows AFM images before and after the incorporation of Ag NPs into a SBS-coated fiber. The SBS-coated fiber before the incorporation of Ag NPs shows a granular surface morphology because of the amorphous configuration caused by chain randomness of the SBS polymer. In the fabrication process of the conductive fiber, the SBS polymer layer is formed by the solution-casting process in ambient room temperature, without controlling the configuration of the SBS polymer. Because of this, the SBS polymer forms amorphous and granular surface morphology (Figure S3a).[26] After repeated Ag NP generation cycles, the conductive fiber includes Ag NPs on the saturated level regardless of its morphology (Figures S1 and S2). After the generation of Ag NPs inside the fiber through the absorption and reduction process of the Ag precursor, the surface of the conductive fiber exhibits a morphology with micro- and nanostructures. This is because Ag NPs form clusters with sizes ranging from several hundreds of nanometers to several micrometers. Owing to this phenomenon, the root mean square roughness of the waterproof conductive fiber rose from 0.675 to 1.171 μm through the incorporation of Ag NPs (Figure S3b).

To characterize SAM-coated conductive fibers, the FT-IR spectra of conductive fibers with different SAMs were obtained (Figure 2b). Every spectrum has a C−C−C in-plane vibration peak at 1229 cm^{-1} and a C−F_2 stretching peak at 1154 cm^{-1}. The C−C−C peak at 1229 cm^{-1} is due to the SBS polymer, which composes the conductive layer of the conductive fiber. The C−F_2 peak at 1154 cm^{-1} is due to the residue from the Ag precursor absorbed in the SBS polymer. However, after the formation of SAMs on the surface of the conductive fiber, the C−C−C peak at 1229 cm^{-1} and the C−F_2 peak at 1154 cm^{-1} are significantly enhanced because of the dense distribution of the C chain of SAM-forming molecules.[22,27−29] In the case of

DOI: 10.1021/acsami.8b10217
ACS Appl. Mater. Interfaces 2018, 10, 36094−36101

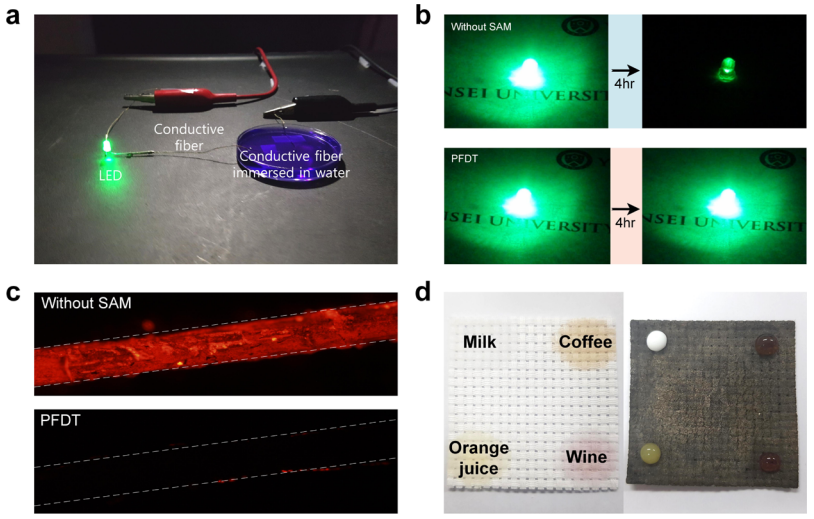

Figure 3. (a) Experimental setting of LED operation of the conductive fiber as an interconnector under water. (b) Comparison of brightness of LED after 4 h of submersion of conductive fibers in water. (c) Confocal fluorescence microscope images of R6G dye on conductive fibers. (d) Formation of the SAM layer-coated Ag NP-SBS polymer composite on a canvas cloth textile and its waterproof and self-cleaning property upon various liquids.

DT, the C−F_2 peak at 1154 cm^{-1} was not observed because of its tail group terminal atom is H, which is in accordance with the contact angle result. In addition, the spectra show tendency with the chain length of carbon atoms. However, there is a difference between FDTS and PFDT, which have the same carbon chain length. Figure 2c shows XPS spectra indicating the peak shift of the Ag binding energy. The spectra show that thiols have larger peak shift than FDTS, which has the silane head group. The amount of shift of binding energy stands for the chemical shift, which is relevant to a stable chemical bonding in the formation of SAMs on Ag NPs.[30] It has been studied that thiolated molecules could form denser and more stable SAMs on the Ag surface compared to SAMs with the silane head group, which results in the superior water repellency of the PFDT-coated conductive fiber among other tested SAMs. In the SAM-forming process, the PFDT compounds are adsorbed onto the surface of Ag NPs within few minutes because of the strong coordination caused by the metal surface-thiol group reaction.[31] Then, the PFDT compounds are crystallized into a two-dimensional unit cell on the surface of metal clusters. The crystallization process is caused by dipole−dipole interactions along the alkyl chain of the PFDT compounds. Because of the close-packed crystalline surface of the PFDT compounds, the PFDT-treated surface exhibits a superhydrophobic property.[31] Figure 2d shows the actual water repelling property of the PFDT-coated conductive fiber. The conductive fiber without the SAM shows submersion into water without any repulsive force. However, the conductive fiber with theSAM of PFDT shows a strong repulsive action on the surface of water.

Figure 2e,f presents the resistance change of SAM-coated conductive fibers according to the water and acid (diluted nitric acid) submersion time. The results show the possibility of a wearable device in watery conditions including weather of acid rain. The pristine conductive fiber and DT SAM-coated conductive fiber shows the increase of resistance according to the submersion time in water. In contrast, the conductive fiber with PFHT, FDTS, and PFDT SAM shows lower resistivity changes than the conductive fiber without SAMs and DT, which are mainly attributed to the lower surface energy of SAMs (Figure S4).[32−34] This result shows that the fluorine (F)-terminated tail group molecules are more suitable for the coating materials for waterproof conductive fibers. Among the F terminated tail group SAMs, PFDT that has longer carbon chain and higher affinity to the surface of conductive fiber shows the least change of resistance in both water and acid. The increase of resistance is due to the oxidation of Ag by acid and water through the following reaction[35,36]

$$2Ag_{(s)} + H_2O_{(l)} \rightarrow Ag_2O_{(s)} + H_{2(g)}$$

When the conductive fiber is immersed in diluted nitric acid with the pH level of acid rain (pH 3), the resistance of the conductive fiber without the SAM increased from 0.11 to 12.8 Ω/cm after 60 min immersion. In this case, Ag NPs are oxidized by the nitric acid through the following reaction.[35,37]

$$2Ag_{(s)} + 4HNO_{3(aq)} \rightarrow Ag_2O_{(s)} + 2HNO_{3(aq)} + 2NO_{2(g)} + H_2O_{(l)}$$

However, as the superhydrophobic surface of the conductive fiber with the PFDT SAM can repel the water and acid solution where the SAM of PFDT acts as an oxidation barrier against water and acid solution.[38] Figure 2g shows the results of XRD of the surface of the bare conductive fiber and conductive fiber with PFDT after 1 h of submersion in diluted nitric acid. As shown in the graph, only the conductive fiber without the SAM exhibited the Ag oxide peaks at 32.1°, 57.4°, 67.4°, 74.4°, and 76.6°.[39,40] With this protective property of the conductive fiber with the PFDT SAM, superior electrical conductivity of the conductive fiber could be maintained longer than the fiber without treatment, which can be potentially applied in advanced E-textile applications.

When operating a wearable device in a watery condition, the degradation of the interconnector caused by a wet operating environment results in malfunction of electrical devices. To confirm the waterproof function and retain electrical conductivity of the PFDT-treated conductive fiber, the operational availability in wet conditions was evaluated by using an LED. Both the conductive fiber without SAM- and

DOI: 10.1021/acsami.8b10217
ACS Appl. Mater. Interfaces 2018, 10, 36094−36101

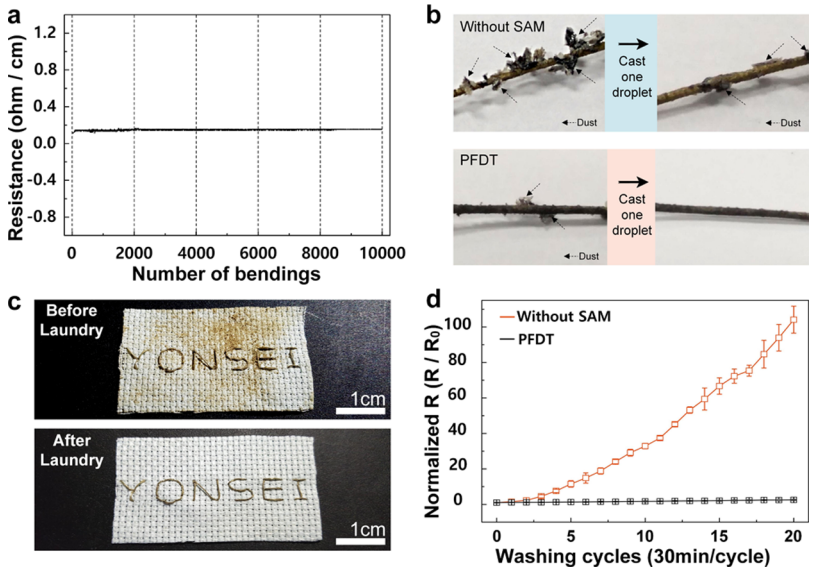

Figure 4. (a) Resistance change of the waterproof conductive fiber after 10 000 times of folding deformation. (b) Self-cleaning property of the PFDT-coated conductive fiber. Dust on the fiber is fully removed by using a single droplet. (c) Photographic image of washable property of conductive fiber weaved into the cotton fabric (upper: before laundry; lower: after laundry). (d) Resistance change of the conductive fibers depending on repeated cycles of washing.

PFTD-treated conductive fiber were used as an interconnector to turn an LED on while immersed in a water-filled dish as shown in Figure 3a,b. At first, both conductive fibers were able to turn the LED on with vivid brightness. However, after 4 h, the brightness of the LED connected to the conductive fiber without the SAM significantly degraded. This is because the immersed part of the conductive fiber without the SAM was oxidized and damaged by the water through the reaction mentioned above. On the other hand, the LED connected to the conductive fiber with the PFDT SAM maintained its brightness for a longer period of time. With the electrical and waterproof performance of the conductive fiber presented, the conductive fiber could be utilized for a waterproof interconnector in varied conditions of operation.

As a waterproof interconnector material for a wearable device, several tests were conducted on the conductive fiber with the PFDT SAM. Figure 3c shows the confocal microscope images of the conductive fiber without the SAM and conductive fiber with PFDT. Each sample is treated with R6G aqueous solution, which has a bright fluorescence effect. The conductive fiber without the SAM shows a bright fluorescence that indicates the fiber being wet by the R6G aqueous solution. In contrast, the conductive fiber with the PFDT SAM shows a dark image without red bright fluorescence, proving great repellency of the R6G aqueous solution, not allowing any adhesion of R6G molecules. On the basis of the results, it can be concluded that the conductive fiber with the PFDT SAM could be protected from the aqueous solution, not only from water but also from other contaminants in solution. In addition, various liquids found in daily life, besides water, were also protected by the PFDT SAM in an operation of fiber-based electric devices. Figure 3d shows the different wetting tendencies to milk, coffee, orange juice, and wine on conductive textiles without the SAM and conductive textile with PFDT. As shown in the figure, conductive textile without the SAM shows stained status by milk, coffee, orange juice, and wine. However, the conductive textile with the PFDT SAM shows sphere-shaped liquids on the surface of textile, which is easily got rid of by wiping with tissue paper. The superhydrophobic nature of the fiber prevents possible malfunction of the conductive textile with the PFDT SAM. This stable operating performance and self-cleanness can assure a safe and clean operating condition as a fundamental interconnection component of wearable devices.

In addition to the high conductivity, the mechanical durability and washability are very important factors for conductive fibers. Figure 4a shows the resistance changes of the fiber upon mechanical folding of the fiber. We observed that the electrical property has not significantly changed (slightly increased from 0.11 to 0.15 Ω/cm) even after repeating 150° folding 10 000 times. This excellent mechanical durability is due to the durable conductive layer formed by the SBS polymer and Ag NPs. Because the SBS polymer containing Ag NPs acts as an elastic and durable scaffold for the connection along the Ag NPs,[9] the conductive pathway can be recovered even after folding deformations. To observe the resistance on the dust or particulate matter, conductive fibers are stained with ash. In Figure 4b, the conductive fiber without the SAM was dirtied by ash dust (upper left) and left behind ash residue after a cleaning process with one droplet of water (upper right). In comparison, ash dust did not attach well on the surface of the conductive fiber with the PFDT SAM (lower left). The conductive fiber with the PFDT SAM also did not leave behind any residue on the surface after a cleaning process with one droplet of water (lower right). Because ofthe superhydrophobicity of the PFDT-treated surface, the conductive fiber with PFDT exhibited a self-cleaning characteristic. This is useful for protection of the surface against dust or particulate contamination for long-term usage as an interconnector.

In addition to the self-cleaning property, washing durability is crucial to keep textile materials clean from being contaminated for subsequent uses. To test the washing durability of the conductive fiber, we sewed the conductive fibers (pristine and PFDT treated) onto a cotton fabric. The conductive fiber fabrics were contaminated with sand dust as

DOI: 10.1021/acsami.8b10217
ACS Appl. Mater. Interfaces 2018, 10, 36094−36101

presented in the Figure 4c. The contaminated fabrics were cleaned for 30 min using a magnetic strirrer with 600 rpm spinning (lower image of Figure 4c). The contaminants were successfully removed after laundry operations. In the conventional laundry process, cotton fabrics are exposed to soapy water and strong splashing motion inside a laundry machine. To investigate the stability in the alkaline soapy water, the resistance change of the conductive fiber without the SAM and conductive fiber with the PFDT SAM was measured (Figure S8). The resistance change in alkalis shows that the conductive fiber does not get significantly affected by the alkaline condition. Figure 4d shows the electrical properties of the conductive fiber without the SAM and the conductive fiber with PFDT before and after repeated washing process cycles. The electrical resistance of the conductive fiber without the SAM increased from 0.11 to 11.44 Ω/cm (10 400% increase) after 20 cycles of washing processes, while the conductive fiber with the PFDT SAM showed a slight change of the resistance (0.11−0.28 Ω/cm). Notably, only the conductive fiber without the SAM was physically damaged during washing processes as the physical durability of the polymer material is degraded because the Ag−polymer composite is fully wetted and swelled during laundry. In addition, the conductive fiber was tested by a standardized test method for textile, AATCC methods, to assess the fiber's resistance to various liquid combinations and ability to release oil stains. For AATCC methods 118, the fiber showed great repellency of liquid combinations including oil, milk, coffee, wine, and orange juice with contact angle ∼150°. The results of AATCC methods 130 indicate that the fabric exhibits the self-cleaning property via removing oil contamination after washing. The test methods, which investigate fabric resistance to the water/IPA solution, AATCC method 193, demonstrated the fabric's feasibility of repelling varying concentrations of the water/IPA solution (Figure S9). Consequently, the conductive fiber with PFDT showed excellent electrical, mechanical, and waterproof ability, which can be widely used as an essential component for an advanced textile interconnector.

4. CONCLUSIONS

In summary, we developed a waterproof conductive fiber with excellent electrical conductivity, mechanical durability, and stability in wet conditions. The waterproof conductive fiber was successfully fabricated by producing a flexible and conductive layer through coating of a rubbery polymer and incorporating Ag NPs inside the polymer. The waterproof conductive fiber exhibited not only an excellent electrical conductivity of 0.11 Ω/cm but also a mechanical durability that was able to withstand folding deformation for 10 000 times. In addition, by forming a SAM of fluorocarbon, which has low surface energy with high affinity to Ag NPs of conductive fiber, we obtained waterproof conductive fibers. The surface of the waterproof conductive fibers exhibited excellent anti-wetting properties without leaving any residue after being submerged into dyed solution, and sustained conductivity even after submersion in water of varying pH values. The waterproof conductive fiber also prevented the Ag NPs inside the conductive layer from being oxidized. As an interconnector for a wearable device, the electrical function of the waterproof conductive fibers was evaluated in harsh and wet conditions. The waterproof conductive fiber exhibited excellent operation of an LED over 4 h through partially immersed conditions. Furthermore, the waterproof conductive fibers were woven into textile and tested under mechanical stress via repeated cycles of washing processes resulting in unchanged conductivity. With the fine self-cleaning performance, the waterproof conductive fiber showed clean surface through AATCC test methods. By considering the advantages of the waterproof conductive fibers presented here, we believe that it can be used as an interconnector in wearable devices.

■ ASSOCIATED CONTENT

Supporting Information

The Supporting Information is available free of charge on the ACS Publications website at DOI: 10.1021/acsami.8b10217.

Resistance change according to the reduction cycle of the Ag NP-SBS polymer composite, TGA analysis of the conductive fiber according to the reduction cycle, AFM analysis of surface of SBS-coated fiber and conductive fiber, and surface energy of DT, PFHT, FDTS, and PFDT (PDF)

Waterproof conductive fiber (PDF)

■ AUTHOR INFORMATION

Corresponding Authors

*E-mail: jungmokseo@kist.re.kr (J.S.).
*E-mail: taeyoon.lee@yonsei.ac.kr (T.L.).

ORCID

Taeyoon Lee: 0000-0002-8269-0257

Notes

The authors declare no competing financial interest.

■ ACKNOWLEDGMENTS

This work was supported by the Priority Research Centers Program (2012-0006689) through the National Research Foundation (NRF) of Korea funded by the Ministry of Education, Science and Technology (MEST) and the R&D program of MOTIE/KEIT [10064081, Development of fiber-based flexible multimodal pressure sensor and algorithm for gesture/posture-recognizable wearable devices]. We gratefully acknowledge the partial support from the National Research Foundation of Korea (NRF-2017M3A7B4049466). This work was also supported by the KIST institutional program (2E27930, 2V06510).

■ REFERENCES

(1) Pradel, K. C.; Wu, W.; Ding, Y.; Wang, Z. L. Solution-Derived ZnO Homojunction Nanowire Films on Wearable Substrates for Energy Conversion and Self-Powered Gesture Recognition. *Nano Lett.* **2014**, *14*, 6897−6905.

(2) Honda, W.; Harada, S.; Arie, T.; Akita, S.; Takei, K. Wearable, Human-Interactive, Health-Monitoring, Wireless Devices Fabricated by Macroscale Printing Techniques. *Adv. Funct. Mater.* **2014**, *24*, 3299−3304.

(3) Zhang, Z.; Chen, X.; Chen, P.; Guan, G.; Qiu, L.; Lin, H.; Yang, Z.; Bai, W.; Luo, Y.; Peng, H. Integrated Polymer Solar Cell and Electrochemical Supercapacitor in a Flexible and Stable Fiber Format. *Adv. Mater.* **2014**, *26*, 466−470.

(4) Inui, T.; Koga, H.; Nogi, M.; Komoda, N.; Suganuma, K. A Miniaturized Flexible Antenna Printed on a High Dielectric Constant Nanopaper Composite. *Adv. Mater.* **2015**, *27*, 1112−1116.

(5) Kennedy, T. F.; Fink, P. W.; Chu, A. W.; Champagne, N. J.; Lin, G. Y.; Khayat, M. A. Body-Worn E-Textile Antennas: The Good, the Low-Mass, and the Conformal. *IEEE Trans. Antennas Propag.* **2009**, *57*, 910−918.

DOI: 10.1021/acsami.8b10217
ACS Appl. Mater. Interfaces 2018, 10, 36094−36101

(6) Castano, L. M.; Flatau, A. B. Smart Fabric Sensors and E-Textile Technologies: a Review. *Smart Mater. Struct.* **2014**, *23*, 053001.
(7) Bonderover, E.; Wagner, S. A Woven Inverter Circuit for e-Textile Applications. *IEEE Electron Device Lett.* **2004**, *25*, 295−297.
(8) Pacelli, M., Loriga, G., Taccini, N., Paradiso, R. Sensing Fabrics for Monitoring Physiological and Biomechanical Variables: E-Textile Solutions. *2006 in 2006 3rd IEEE/EMBS International Summer School on Medical Devices and Biosensors, ISSS-MDBS*, 2006.
(9) Lee, J.; Kwon, H.; Seo, J.; Shin, S.; Koo, J. H.; Pang, C.; Son, S.; Kim, J. H.; Jang, Y. H.; Kim, D. E.; Lee, T. Conductive Fiber-based Ultrasensitive Textile Pressure Sensor for Wearable Electronics. *Adv. Mater.* **2015**, *27*, 2433−2439.
(10) Lee, S.; Shin, S.; Lee, S.; Seo, J.; Lee, J.; Son, S.; Cho, H. J.; Algadi, H.; Al-Sayari, S.; Kim, D. E.; Lee, T. Ag Nanowire Reinforced Highly Stretchable Conductive Fibers for Wearable Electronics. *Adv. Funct. Mater.* **2015**, *25*, 3114−3121.
(11) Yu, L.-h.; Wang, R.; Xu, L.; Tao, Q. Preparation of MWCNTs/CuPc/Ag modified conductive polyester fiber with chemical liquid deposition. *J. Mater. Sci.: Mater. Electron.* **2016**, *27*, 1416−1420.
(12) Liu, X.; Guo, R.; Shi, Y.; Deng, L.; Li, Y. Durable, Washable, and Flexible Conductive PET Fabrics Designed by Fiber Interfacial Molecular Engineering. *Macromol. Mater. Eng.* **2016**, *301*, 1383−1389.
(13) Jianming, J.; Wei, P.; Shenglin, Y.; Guang, L. Electrically Conductive PANI-DBSA/Co-PAN Composite Fibers Prepared by Wet Spinning. *Synth. Met.* **2005**, *149*, 181−186.
(14) Xu, R.; Wei, J.; Guo, F.; Cui, X.; Zhang, T.; Zhu, H.; Wang, K.; Wu, D. Highly conductive, twistable and bendable polypyrrole-carbon nanotube fiber for efficient supercapacitor electrodes. *RSC Adv.* **2015**, *5*, 22015−22021.
(15) Lim, T. H.; Lee, S. H.; Yeo, S. Y. Highly Conductive Polymer/Metal/Carbon Nanotube Composite Fiber Prepared by the Melt-Spinning Process. *Text. Res. J.* **2016**, *87*, 593−606.
(16) Yang, Y.; Huang, Q.; Huang, Q.; Niu, L.; Wang, D.; Yan, C.; She, Y.; Zheng, Z. Waterproof, Ultrahigh Areal-Capacitance, Wearable Supercapacitor Fabrics. *Adv. Mater.* **2017**, *29*, 1606679.
(17) Coclite, A. M.; Howden, R. M.; Borrelli, D. C.; Petruczok, C. D.; Yang, R.; Yagüe, J. L.; Ugur, A.; Chen, N.; Lee, S.; Jo, W. J.; Liu, A.; Wang, X.; Gleason, K. K. 25th Anniversary Article: CVD Polymers: A New Paradigm for Surface Modifi cation and Device Fabrication. *Adv. Mater.* **2013**, *25*, 5392−5423.
(18) Soto, D.; Ugur, A.; Farnham, T. A.; Gleason, K. K.; Varanasi, K. K. Short-Fluorinated iCVD Coatings for Nonwetting Fabrics. *Adv. Funct. Mater.* **2018**, *28*, 1707355.
(19) Wu, X.; Han, Y.; Zhang, X.; Lu, C. Highly Sensitive, Stretchable, and Wash-Durable Strain Sensor Based on Ultrathin Conductive Layer@Polyurethane Yarn for Tiny Motion Monitoring. *ACS Appl. Mater. Interfaces* **2016**, *8*, 9936−9945.
(20) Jeon, J. W.; Cho, S. Y.; Jeong, Y. J.; Shin, D. S.; Kim, N. R.; Yun, Y. S.; Kim, H.-T.; Choi, S. B.; Hong, W. G.; Kim, H. J.; Jin, H.; Kim, B. Pyroprotein-Based Electronic Textiles with High Stability. *Adv. Mater.* **2017**, *29*, 1−6.
(21) Park, M.; Im, J.; Shin, M.; Min, Y.; Park, J.; Cho, H.; Park, S.; Shim, M.-B.; Jeon, S.; Chung, D.-Y.; Bae, J.; Park, J.; Jeong, U.; Kim, K. Highly Stretchable Electric Circuits from a Composite Material of Silver Nanoparticles and Elastomeric Fibres. *Nat. Nanotechnol.* **2012**, *7*, 803−809.
(22) Battocchio, C.; Meneghini, C.; Fratoddi, I.; Venditti, I.; Russo, M. V.; Aquilanti, G.; Maurizio, C.; Bondino, F.; Matassa, R.; Rossi, M.; Mobilio, S.; Polzonetti, G. Silver Nanoparticles Stabilized with Thiols: A Close Look at the Local Chemistry and Chemical Structure. *J. Phys. Chem. C* **2012**, *116*, 19571−19578.
(23) Chandekar, A.; Sengupta, S. K.; Whitten, J. E. Thermal Stability of Thiol and Silane Monolayers: A Comparative Study. *Appl. Surf. Sci.* **2010**, *256*, 2742−2749.
(24) Seo, J.; Lee, S.-K.; Lee, J.; Lee, J. S.; Kwon, H.; Cho, S.-W.; Ahn, J.-H.; Lee, T. Path-Programmable Water Droplet Manipulations on an Adhesion Controlled Superhydrophobic Surface. *Sci. Rep.* **2015**, *5*, 12326.
(25) Seo, J.; Lee, J. S.; Lee, K.; Kim, D.; Yang, K.; Shin, S.; Mahata, C.; Jung, H. B.; Lee, W.; Cho, S.-W.; Lee, T. Switchable Water-Adhesive, Superhydrophobic Palladium-Layered Silicon Nanowires Potentiate the Angiogenic Efficacy of Human Stem Cell Spheroids. *Adv. Mater.* **2014**, *26*, 7043−7050.
(26) Romero-Sánchez, M. D.; Pastor-Blas, M. M.; Martín-Martínez, J. M. Treatment of a Styrene-Butadiene-Styrene Rubber with Corona Discharge to Improve the Adhesion to Polyurethane Adhesive. *Int. J. Adhes. Adhes.* **2003**, *23*, 49−57.
(27) Lu, F., Jin, M., Belkin, M. A. Mid-Infrared Absorption Nanospectroscopy Via Molecular Force Detection. *CLEO: QELS_-Fundamental Science*, 2013; Vol. *1*, p 1.
(28) Alves, C. A.; Porter, M. D. Atomic Force Microscopic Characterization of a Fluorinated Alkanethiolate Monolayer at Gold and Correlations to Electrochemical and Infrared Reflection Spectroscopic Structural Descriptions. *Langmuir* **1993**, *9*, 3507−3512.
(29) Lenk, T. J.; Hallmark, V. M.; Hoffmann, C. L.; Rabolt, J. F.; Castner, D. G.; Erdelen, C.; Ringsdorf, H. Structural Investigation of Molecular Organization in Self-Assembled Monolayers of a Semi-fluorinated Amidethiol. *Langmuir* **1994**, *10*, 4610−4617.
(30) Han, S. W.; Kim, Y.; Kim, K. Dodecanethiol-Derivatized Au/Ag Bimetallic Nanoparticles: TEM, UV/VIS, XPS, and FTIR Analysis. *J. Colloid Interface Sci.* **1998**, *208*, 272−278.
(31) Ulman, A. Formation and Structure of Self-Assembled Monolayers. *Chem. Rev.* **1996**, *96*, 1533−1554.
(32) Fischer, D.; Curioni, A.; Andreoni, W. Decanethiols on Gold: The Structure of Self-Assembled Monolayers Unraveled with Computer Simulations. *Langmuir* **2003**, *19*, 3567−3571.
(33) Lamprou, D. A.; Smith, J. R.; Nevell, T. G.; Barbu, E.; Stone, C.; Willis, C. R.; Tsibouklis, J. A Comparative Study of Surface Energy Data From Atomic Force Microscopy and from Contact Angle Goniometry. *Appl. Surf. Sci.* **2010**, *256*, 5082−5087.
(34) Janssen, D.; De Palma, R.; Verlaak, S.; Heremans, P.; Dehaen, W. Static Solvent Contact Angle Measurements, Surface Free Energy and Wettability Determination of Various Self-Assembled Monolayers on Silicon Dioxide. *Thin Solid Films* **2006**, *515*, 1433−1438.
(35) Chudnovsky, B. H. Degradation of Power Contacts in Industrial Atmosphere: Silver Corrosion and Whiskers. *Proceedings of the Forty-Eighth IEEE Holm Conference on Electrical Contacts*, 2002; Vol. *1*, pp 140−150.
(36) Setoura, K.; Ito, S.; Yamada, M.; Yamauchi, H.; Miyasaka, H. Fabrication of Silver Nanoparticles from Silver Salt Aqueous Solution at Water-Glass Interface by Visible CW Laser Irradiation without Reducing Reagents. *J. Photochem. Photobiol., A* **2017**, *344*, 168−177.
(37) Nie, S.; Liu, C.; Zhang, Z.; Liu, Y. Nitric Acid-Mediated Shape-Controlled Synthesis and Catalytic Activity of Silver Hierarchical Microcrystals. *RSC Adv.* **2016**, *6*, 21511−21516.
(38) Xia, Y.; Zhao, X.-M.; Whitesides, G. M. Pattern transfer: Self-assembled monolayers as ultrathin resists. *Microelectronic Engineering* **1996**, *32*, 255−268.
(39) Waterhouse, G. I. N.; Bowmaker, G. A.; Metson, J. B. The Thermal Decomposition of Silver (I, III) Oxide: A Combined XRD, FT-IR and Raman Spectroscopic Study. *Phys. Chem. Chem. Phys.* **2001**, *3*, 3838−3845.
(40) Gao, X.-Y.; Wang, S.-Y.; Li, J.; Zheng, Y.-X.; Zhang, R.-J.; Zhou, P.; Yang, Y.-M.; Chen, L.-Y. Study of Structure and Optical Properties of Silver Oxide Films by Ellipsometry, XRD and XPS Methods. *Thin Solid Films* **2004**, *455*−*456*, 438−442.

DOI: 10.1021/acsami.8b10217
ACS Appl. Mater. Interfaces 2018, 10, 36094−36101